Comparative models for diffusion of implanted beryllium in gallium arsenide

2006 J. Phys.: Condens. Matter 18 L283

(http://iopscience.iop.org/0953-8984/18/22/L02)

INSTITUTE OF PHYSICS PUBLISHING JOURNAL OF PHYSICS: CONDENSED MATTER

J. Phys.: Condens. Matter **18** (2006) L283–L288 doi:10.1088/0953-8984/18/22/L02

LETTER TO THE EDITOR

Comparative models for diffusion of implanted beryllium in gallium arsenide

S Koumetz[1], J-C Pesant[2] and C Dubois[3]

[1] GPM, UMR CNRS 6634, Technopôle du Madrillet, 76800 Saint Etienne du Rouvray, France
[2] IEMN, UMR CNRS 8520, Cité Scientifique, 59652 Villeneuve d'Ascq, France
[3] LPM, UMR CNRS 5511, 7 avenue Jean Capelle, 69621 Villeurbanne, France

Received 25 November 2005, in final form 27 April 2006
Published 16 May 2006
Online at stacks.iop.org/JPhysCM/18/L283

Abstract

The diffusion of implanted Be in GaAs at 100 keV for doses of 1×10^{13} cm^{-2} and 1×10^{14} cm^{-2} has been investigated. The observed secondary ion mass spectrometry profiles, obtained for annealing temperatures of 700–900 °C and anneal times from 60 to 240 s, were simulated using different models of the kick-out mechanism and taking into account the 'plus one' approach for Ga self-interstitial generation after implantation as well as the local Ga self-interstitial sink phenomenon. The diffusion differential equations for Be and Ga mobile species with initial and boundary conditions were solved numerically for each model by using the explicit finite-difference method.

1. Introduction

Ion-implanted beryllium is an efficient p-type dopant in gallium arsenide. Due to its light mass, Be can be precisely implanted over a wide range of depths, and it produces less damage than other acceptor species. However, implanted Be manifests anomalous diffusion behaviour during annealing which needs to be understood.

Investigations on the diffusion mechanisms of implanted beryllium in gallium arsenide in comparison with studies of grown-in Be diffusion behaviour in GaAs [1–4] are still limited [5, 6]. Nevertheless, variations on the kick-out mechanism [1] have been put forward to account for the data [5, 6].

In this letter we describe results on Be diffusion in GaAs during post-implant rapid thermal annealing (RTA) using three models of kick-out mechanism.

2. Experimental procedure

Undoped semi-insulating ⟨100⟩ oriented liquid-encapsulated Czochralski-grown (LEC) GaAs wafers from Freiberger were implanted at room temperature with Be^+ ions at an energy of 100 keV and doses of 1×10^{13} and 1×10^{14} cm^{-2} in an Eaton 3204 system.

The post-implant RTA was performed for 1–4 min at temperatures of 700–900 °C in a halogen-lamp furnace, Jetstar 100S from Jipelec, using 15% $H_2 + N_2$ flowing forming gas.

Secondary ion mass spectrometry (SIMS) depth profiling was carried out with a Cameca IMS-4F instrument using an O_2^+ primary ion beam with an energy of 8 keV and an intensity of 300 nA rastered over a 250 × 250 μm^2 area. The secondary ions were collected from an area 60 μm in diameter with a mass resolving power of 300. The depths of the SIMS craters were measured using a P10 KLA-Tencor surface profilometer with an accuracy of about 5%.

3. Diffusion mechanism

It is well recognized that beryllium is an interstitial–substitutional species in gallium arsenide, and according to most authors [1–6], the conversion of Be between a substitutional and an interstitial site is generally considered to proceed via the kick-out mechanism [1], consistent with its effect on superlattice disordering [7]:

$$\mathrm{Be}_i^{j+} \underset{k_b}{\overset{k_f}{\Leftrightarrow}} \mathrm{Be}_s^- + \mathrm{I}_{Ga}^{n+} + (1 + j - n)\mathrm{h}^+ \tag{1}$$

where Be_s^- is an active Be substitutional anion, Be_i^{j+} is a Be interstitial with charge j, I_{Ga}^{n+} is a Ga self-interstitial with charge n, h^+ represents a free hole, and k_f and k_b denote the forward and backward rate constants, respectively.

From the analyses of Be diffusion near the p/n junction as well as the concentration dependence of Be diffusivity and also from the simulation studies, values of 0 [5, 8] and +1 [3, 4, 6, 9] have been proposed for Be interstitial charge.

Based on calculations of the Ga self-interstitial formation energy [10, 11], superlattice disordering experiments [12] and the simulation results [3–6, 13, 14], different groups have concluded that the charge state of Ga self-interstitials in GaAs is 0 [5], +1 [3, 4, 6], +2 [1, 2, 12], +2 and +3 [12, 13], 0 and +1 [14].

4. Results and discussions

The anomalous diffusion behaviour of implanted Be [5, 6], relative to the diffusion profile shapes, has been mainly observed for a high dose during a low-temperature RTA in our experiments. According to the 'plus one' approach [15], it has been attributed essentially to the strong excess of Ga interstitial point defects generated by the Be implanted ions going onto substitutional lattice sites via a kick-out mechanism, as soon as the annealing begins, in addition to the Ga interstitials created by the smaller knock-on process during ion implantation [6]. In this way, the last process was neglected [6] and the initial excess Ga self-interstitial profile has been identical to the corresponding as-implanted Be ion distribution for each dose in our simulations [6, 15].

It has been assumed also that there is the Ga local interstitial sink region, of depth x_I, from the sample surface to just beyond a mean projected range distance R_p below the surface, which absorbs the Ga interstitial excess with a rate proportionate to the latter [6].

To obtain quantitative data fits with a complete set of parameters [16], three kick-out models have been studied.

The first model is based on singly positively charged Be interstitials Be_i^+ and singly positively charged Ga self-interstitials I_{Ga}^+; that is: $j = 1$ and $n = 1$ in reaction (1) [3, 4, 6]. The second model involves also Be_i^+ species and doubly positively ionized Ga self-interstitial species I_{Ga}^{2+}: $j = 1$ and $n = 2$ [1, 2]. The third model is composed of two diffusion reactions: the reaction of the second model and the reaction involving doubly positively charged Be interstitials Be_i^{2+} and triply positively charged Ga self-interstitials I_{Ga}^{3+} [13] ($j = 2$ and $n = 3$).

The SIMS as-implanted depth profiles have been used as the initial Be concentration distributions in our simulations [5, 6, 15]. In all models, we assumed a detailed balance between the species involved in the kick-out reactions (1) [1–6]. In this way, the reaction constant $K = k_b/k_f$, given by the law of mass action applied to the corresponding diffusion reactions under thermal equilibrium conditions, has been used in all locations for all times in the first and the second models [1, 2, 16]. In the third model, the backward rate constant values have been imposed while the forward rate constants have been eliminated in our equations using the principle of detailed balance applied to the associated diffusion reactions [14]. The diffusion differential equations for Be and Ga mobile species were solved numerically for each model by a finite-difference algorithm [16, 18] taking into account the Fermi-level effect [7], the built-in electric field phenomenon [1, 2] and using the surface boundary conditions for Be [17] and Ga [3] mobile species. The obtained algebraic equations of the fourth degree for the Be concentration in the first model were solved for all locations and all times using Bairstow's numerical method [19]. The values of the intrinsic carrier concentration n_i for different temperatures were calculated [20]. The other diffusion parameters, such as the ratio of the Be equilibrium interstitial concentration to the Be equilibrium substitutional concentration $r = C_i^{eq}/C_s^{eq}$ [4] for a Be peak concentration, the rate coefficient of Ga self-interstitial annihilation at the local interstitial sinks k_I [6], the out-diffusion rate of Be interstitials ν_i [17], the surface recombination constant of Ga self-interstitials ν_I [3], the intrinsic equilibrium concentration of Ga self-interstitials $C_I^{eq}(n_i)$, the Be interstitial diffusivity D_i and the Ga self-interstitial diffusivity D_I (the last three of them as a function of temperature [16]) were optimized to give a best fit to the experimental profiles obtained for a high dose of 1×10^{14} cm^{-2}. In the modelling of Be SIMS curves, obtained for a low dose of 1×10^{13} cm^{-2}, we used the same values of the parameters ν_i, ν_I, x_I, $C_I^{eq}(n_i)$, D_i, D_I, and the equilibrium concentration ratios r were calculated from the same values of the reaction constant K [4].

In this study, the considered models provided a fairly good fit to the experimental profiles. The third model gave very good simulation results for Be distribution in the samples with a dose of 1×10^{14} cm^{-2} that were annealed for 60–240 s at a temperature of 700 °C, as is shown in figure 1.

The simulations of Be diffusion taking place under other experimental conditions gave approximately equivalent results for these three models, as, for example, in the case of a dose of 1×10^{13} cm^{-2} and an annealing at 800 °C for 180 s, illustrated in figure 2.

By way of example, the parameter values used for two implanted doses by the first model are listed in table 1. The intrinsic equilibrium concentration values of Ga self-interstitials $C_I^{eq}(n_i)$ are close to those obtained by Hu *et al* [6]: 7.5×10^{11}, 3.5×10^{12} and 8.0×10^{13} cm^{-3} for 700, 800 and 900 °C respectively, and by Mosca *et al* [4]: 3.1×10^{13} cm^{-3} at a temperature of 850 °C. The differences between our Ga self-interstitial diffusivity D_I values and those reported in [6]: 7.5×10^{-12} and 3.0×10^{-11} cm^2 s^{-1} for 700 and 800 °C respectively, are less than an order of magnitude. However, our Be interstitial diffusivity D_i value for 850 °C is an order of magnitude larger then that given in [4]: 4.8×10^{-11} cm^2 s^{-1}. It should be noted that the $C_I^{eq}(n_i)$, D_i, D_I and reaction constant K values, listed in table 1, satisfy the Arrhenius law for all studied temperatures:

$$C_I^{eq}(n_i) = 3.47 \times 10^{25} \exp(-2.74\, eV/k_B T) \text{ cm}^{-3},$$

$$D_i = 3.10 \exp(-2.17\, eV/k_B T) \text{ cm}^2 \text{ s}^{-1},$$

$$D_I = 1.61 \exp(-2.14\, eV/k_B T) \text{ cm}^2 \text{ s}^{-1}, \qquad K = 1.55 \times 10^{-45} \exp(1.72\, eV/k_B T) \text{ cm}^6$$

which shows a certain reliability of the obtained values in this example.

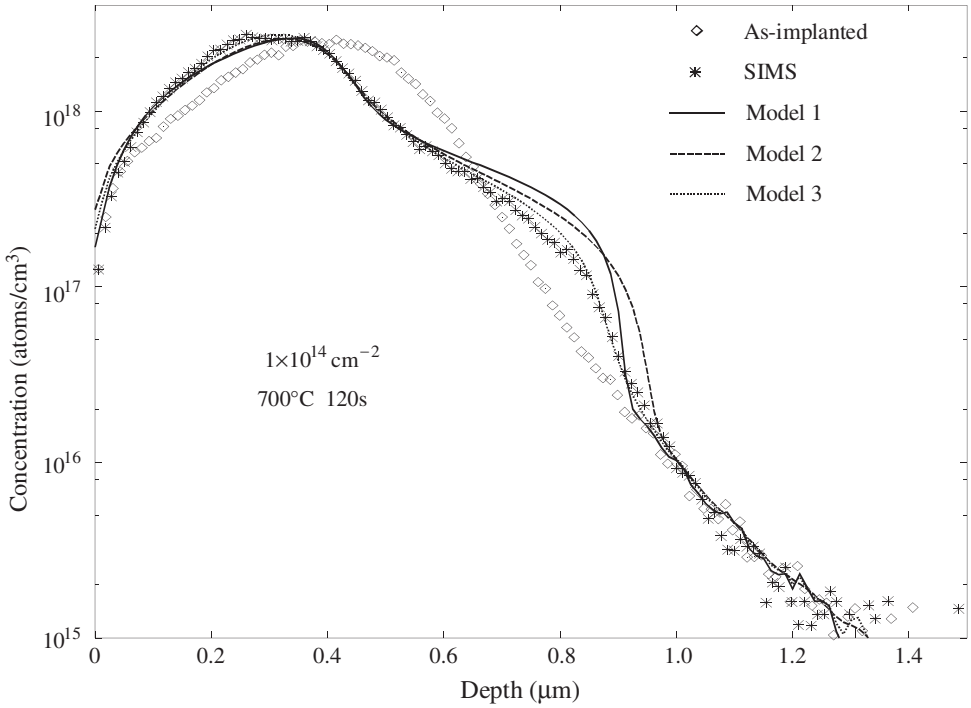

Figure 1. The Be SIMS data and simulated results for a dose of 1×10^{14} cm^{-2} and an annealing at 700 °C for 120 s.

Table 1. The parameter values used for the simulations by the first model.

RTA	$C_I^{eq}(n_i)$	D_i	D_I	k_I (s^{-1})		K	n_i
T (°C)	(cm^{-3})	(cm^2 s^{-1})	(cm^2 s^{-1})	Low-dose	High-dose	(cm^6)	(cm^{-3})
700	2.3×10^{11}	1.8×10^{-11}	1.4×10^{-11}		7.2×10^{-1}	1.2×10^{-36}	2.5×10^{16}
750	1.1×10^{12}	6.4×10^{-11}	4.9×10^{-11}	8.0×10^{-2}	8.0×10^{-1}	4.4×10^{-37}	4.6×10^{16}
800	4.8×10^{12}	2.0×10^{-10}	1.5×10^{-10}	1.0×10^{-1}	8.8×10^{-1}	1.8×10^{-37}	7.9×10^{16}
850	1.8×10^{13}	5.7×10^{-10}	4.2×10^{-10}	1.2×10^{-1}	9.6×10^{-1}	7.8×10^{-38}	1.3×10^{17}
900	6.0×10^{13}	1.5×10^{-9}	1.1×10^{-9}	1.5×10^{-1}		3.7×10^{-38}	2.0×10^{17}

$R_p = 0.40$ μm, $x_I = 0.45$ μm, $\nu_i = 2 \times 10^{-5}$ cm s^{-1}, $\nu_I = 1 \times 10^{-6}$ cm s^{-1}, $r = 6.3 \times 10^{-5}$ for the high dose, $r \approx 1.0 \times 10^{-6}$ for the low dose.

For the samples with a Be dose of 1×10^{14} cm^{-2} annealed at 700 °C for all the anneal times, the Be profiles show a small transient uphill diffusion behaviour [5, 6] and an asymmetric kink and tail feature [6], as can be seen in figure 1. These anomalous phenomena, as well as a diffusion enhancement taking place during the initial stage of RTA [5, 6, 15], have been explained in our modelling by the strong excess of Ga self-interstitials mainly generated by the kick-out mechanism at the beginning of annealing [6, 15].

5. Conclusions

In this work, the diffusion of implanted Be in undoped GaAs taking place during RTA has been fairly well described on the basis of the kick-out mechanism involving singly positively

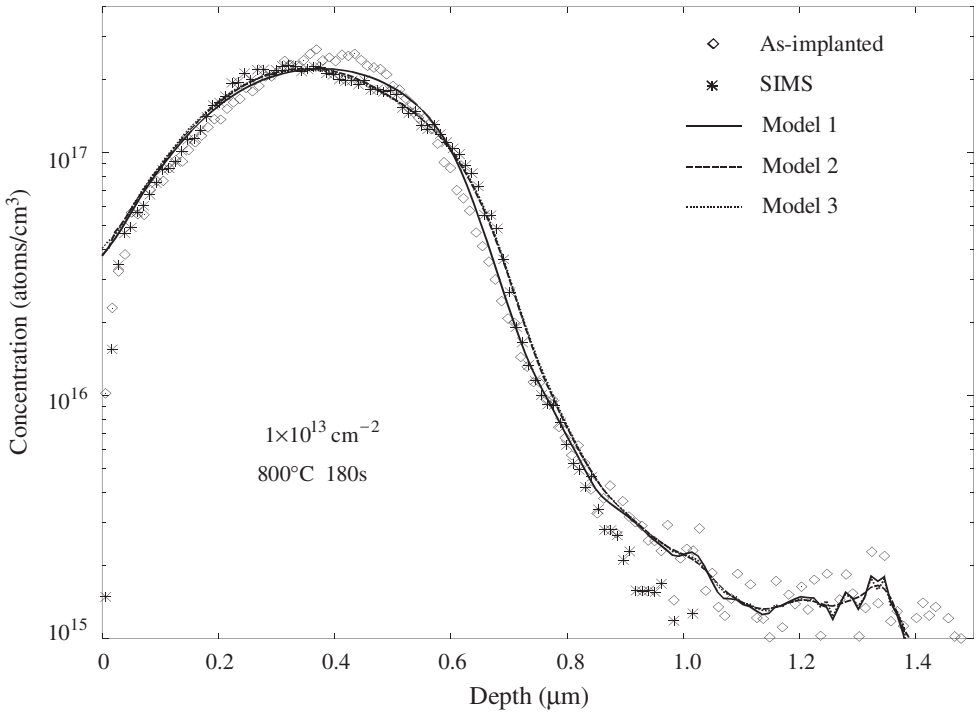

Figure 2. The Be SIMS data and simulated results for a dose of 1×10^{13} cm^{-2} and an annealing at 800 °C for 180 s.

charged Be and Ga interstitials in the first model, singly positively charged Be interstitials and doubly positively charged Ga interstitials in the second model, singly and doubly positively charged Be interstitials with doubly and triply positively charged Ga interstitials, respectively, in the third model.

We obtained approximately equivalent fits to the experimental profiles using these models; nevertheless, it must be noted that the Be diffusion taking place in the implanted samples with a Be dose of 1×10^{14} cm^{-2} during a low-temperature annealing at 700 °C for all the annealing times has been most accurately simulated by the third model.

The authors are grateful to Laurent Fugere of the IEMN laboratories of Lille for carrying out the implantations and the annealing processes. We would also like to thank Fabrice Lefebvre of the University of Rouen for generously providing the SIMS software.

References

[1] Yu S, Tan T Y and Gösele U 1991 *J. Appl. Phys.* **69** 3547
[2] Uematsu M, Wada K and Gösele U 1992 *Appl. Phys.* A **55** 301
[3] Hu J C, Deal M D and Plummer J D 1995 *J. Appl. Phys.* **78** 1595
[4] Mosca R, Bussei P, Franchi S, Frigeri P, Gombia E, Carnera A and Peroni M 2003 *J. Appl. Phys.* **93** 9709
[5] Deal M D and Robinson H G 1989 *Solid-State Electron.* **33** 665
[6] Hu J C, Deal M D and Plummer J D 1995 *J. Appl. Phys.* **78** 1606
[7] Tan T Y and Gösele U 1988 *Mater. Sci. Eng.* B **1** 47
[8] Masu K, Nakatsuka S, Konagai M and Takahashi K 1982 *J. Electrochem. Soc.* **129** 1623
[9] Enquist P, Wicks G W, Eastman L F and Hitzman C 1985 *J. Appl. Phys.* **58** 4130

[10] Jansen R W, Wolde-Kidane D S and Sankey O F 1988 *J. Appl. Phys.* **64** 2415
[11] Zhang S B and Northrup J E 1991 *Phys. Rev. Lett.* **67** 2339
[12] Zucker E P, Hashimoto A, Fukunaga T and Watanabe N 1989 *Appl. Phys. Lett.* **54** 564
[13] Bösker G, Stolwijk N A, Hettwer H-G, Rucki A, Jäger W and Södervall U 1995 *Phys. Rev.* B **52** 11927
[14] Bracht H and Brotzmann S 2005 *Phys. Rev.* B **71** 115216
[15] Giles M D 1991 *J. Electrochem. Soc.* **138** 1160
[16] Koumetz S and Dubois C 2003 *J. Cryst. Growth* **252** 14
[17] Ortiz C, Grob J J, Mathiot D, Claverie A, Dubois C and Jérisian R 1999 *Nucl. Instrum. Methods Phys. Res.* B **147** 122
[18] Crank J 1956 *The Mathematics of Diffusion* (Oxford: Oxford University Press)
[19] Nougier J P 1987 *Méthodes de Calcul Numérique* (Paris: Masson)
[20] Blakemore J S 1982 *J. Appl. Phys.* **53** 520